Environmental Science
Processes & Impacts

ROYAL SOCIETY
OF CHEMISTRY

PAPER
Jiří Kalina, Kevin B. White *et al.*
Comparability of semivolatile organic compound
concentrations from co-located active and passive
air monitoring networks in Europe

ROYAL SOCIETY
OF CHEMISTRY

PAPER

Check for updates

Comparability of semivolatile organic compound concentrations from co-located active and passive air monitoring networks in Europe†

Jiří Kalina,[a] Kevin B. White, [ID] [a] Martin Scheringer, [ID] *[ab] Petra Přibylová,[a] Petr Kukučka,[a] Ondřej Audy,[a] Jakub Martiník[a] and Jana Klánová*[a]

Passive air sampling (PAS) has been used to monitor semivolatile organic compounds (SVOCs) for the past 20 years, but limitations and uncertainties persist in the derivation of effective sampling volumes, sampling rates, and concentrations. As a result, the comparability of atmospheric levels measured by PAS and concentrations measured by active air sampling (AAS) remains unclear. Long-term PAS data, without conversion into concentrations, provide temporal trends that are similar to, and consistent with, trends from AAS data. However, for more comprehensive environmental and human health assessments of SVOCs, it is also essential to harmonize and pool air concentration data from the major AAS and PAS monitoring networks in Europe. To address this need, we calculated and compared concentration data for 28 SVOCs (including organochlorine pesticides (OCPs), polychlorinated biphenyls (PCBs), polybrominated diphenyl ethers (PBDEs), and polycyclic aromatic hydrocarbons (PAHs)) at the six monitoring sites in Europe with 10 years of co-located AAS (EMEP) and PAS (MONET) data: Birkenes, Košetice, Pallas, Råö, Stórhöfði, and Zeppelin. Atmospheric SVOC concentrations were derived from PAS data using the two most common computation models. Long-term agreement between the AAS and PAS data was strong for most SVOCs and sites, with 79% of the median PAS-derived concentrations falling within a factor of 3 of their corresponding AAS concentrations. However, in both models it is necessary to set a sampler-dependent correction factor to prevent underestimation of concentrations for primarily particle-associated SVOCs. In contrast, the models overestimate concentrations at sites with wind speeds that consistently exceed 4 m s^{-1}. We present two recommendations that, if followed, allow MONET PAS to provide sufficiently accurate estimates of SVOC concentrations in air so that they can be deployed together with AAS in regional and global monitoring networks.

Environmental significance

Active air sampling (AAS) has historically been used to measure atmospheric concentrations of semivolatile organic compounds (SVOCs) but is impractical for long-term monitoring in most regions of the world. Passive air sampling (PAS) is a more feasible alternative, but after 20 years of combined global air monitoring, the comparability of concentration data between AAS and PAS is still unclear. However, data harmonization and pooling between major AAS and PAS monitoring networks is essential for evaluating the effectiveness of global regulations and the impacts of SVOCs on environmental and human health. Our study identifies strong agreement between 10 years of co-located AAS and PAS concentrations in most cases and confirms the potential for harmonization and pooling of SVOC air monitoring data.

Introduction

Semivolatile organic compounds (SVOCs) are a broad class of atmospheric pollutants that include polycyclic aromatic hydrocarbons (PAHs) and persistent organic pollutants (POPs),

[a]RECETOX, Faculty of Science, Masaryk University, Kotlarska 2, 611 37 Brno, Czech Republic. E-mail: martin.scheringer@recetox.muni.cz; jana.klanova@recetox.muni.cz
[b]Institute of Biogeochemistry and Pollutant Dynamics, ETH Zürich, 8092 Zürich, Switzerland. E-mail: scheringer@usys.ethz.ch
† Electronic supplementary information (ESI) available. See https://doi.org/10.1039/d2em00007e

such as polychlorinated biphenyls (PCBs), organochlorine pesticides (OCPs), and polybrominated diphenyl ethers (PBDEs). Within Europe, SVOCs have been monitored since the 1990s at active air sampling (AAS) sites under the European Monitoring and Evaluation Programme (EMEP) (Norwegian Institute for Air Research, NILU).[1] Baseline concentrations were established across the continent, but continuous long-term monitoring of SVOCs is primarily performed at sites in Northern and Western Europe. In 2003, the MONET passive air sampling (PAS) network was established by RECETOX (Masaryk University, Czech Republic) to address SVOC monitoring gaps

898 | *Environ. Sci.: Processes Impacts*, 2022, **24**, 898–909

This journal is © The Royal Society of Chemistry 2022

in Central and Eastern Europe.[2] The network has since expanded, with MONET PAS now deployed in 27 countries across Europe, as well as 9 countries across Africa,[3] and generating valuable information on the atmospheric behavior of SVOCs.[4–6] However, the comparability between atmospheric levels measured by PAS and atmospheric concentrations measured by AAS remains the subject of ongoing investigation and discussion.[7–11]

There are several methods for converting atmospheric levels of SVOCs measured by the most common kinetic PAS (mass per sampler) into atmospheric concentrations as those measured by AAS (mass per volume of sampled air), all of which are based on the concept of sampling rate (R_S). The R_S quantitatively describes the uptake of SVOCs by PAS and is dependent on compound-specific chemical properties, as well as local meteorological conditions such as wind speed, pressure, humidity, and temperature.[12] Methods for the determination of R_S range from site-specific field calibrations based on parallel AAS and PAS deployment or the use of sampler depuration compounds,[13] to physicochemical models aiming for broad applicability.[7] While the role of temperature in SVOC uptake has generally been well understood since the advent of PAS,[14] many studies have attempted to elucidate the influence of other meteorological parameters, particularly wind speed.[15–21] Models based on these uptake relationships – such as the original GAPS template by Harner[22] and the newer GAPS model by Herkert *et al.*[23] – provide acceptable air concentration estimates for the majority of sampling sites under typical meteorological conditions, but larger differences between modelled and field-based R_S may be observed at sites that experience extreme temperatures and/or wind speeds.[8,23] This indicates that the relationship between meteorological factors and SVOC uptake is still not satisfactorily described. For example, wind speeds above a certain threshold may cause a transition from laminar to turbulent flow inside passive samplers, which significantly increases R_S and is not reflected in current models.[12,15,18]

We have previously shown that SVOC concentrations from co-located EMEP AAS and MONET PAS monitoring sites provide similar long-term temporal trends despite differences in individual sample values and units between the networks.[4,9] However, there is also a need to harmonize AAS and PAS monitoring results with respect to absolute SVOC air concentrations in order to generate consistent data across Europe for more robust environmental and human exposure assessments. We have also previously described sources of uncertainty and challenges for the harmonization of AAS and PAS SVOC air sampling, such as differences in sampler design,[11,24,25] including potentially problematic artifacts,[4,26] as well as differences in analytical performance between laboratories generating global SVOC air monitoring data.[27] This study focuses on the final source of uncertainty for harmonization of AAS and PAS data – the determination of R_S – using ten years (2009–2018) of continuous air monitoring data for PAHs, PCBs, OCPs, and PBDEs from the six sites in Europe with co-located EMEP AAS and MONET PAS to derive field-based R_S and compare them with results from the most commonly used models[22,23] for R_S determination. This comparison enables us to address the

challenge of reducing the uncertainties of PAS data[7] to improve the potential for harmonization of SVOC air monitoring data across Europe.

Methods

Air sampling and chemical analysis

The six air monitoring stations across Europe with long-term co-located EMEP AAS and MONET PAS are Birkenes (Norway), Košetice (Czech Republic), Pallas (Finland), Råö (Sweden), Stórhöfði (Iceland), and Zeppelin (Svalbard, Norway). For the purposes of this study, we investigated a decade of concurrent monitoring data from both networks at these sites (1-January-2009 to 31-December-2018) obtained from the publicly available EMEP (EBAS, NILU) and MONET (Genasis, RECETOX) databases. Compound selection was constrained to the 24 SVOCs monitored by both networks at all (or most) of the six sites over the selected period: alpha- and gamma-hexachlorocyclohexane (α-HCH, γ-HCH), hexachlorobenzene (HCB), and p,p'-dichlorodiphenyldichloroethylene (p,p'-DDE); PCBs 28, 52, 101, 118, 138, 153, and 180; fluoranthene (FLA), fluorene (FLU), phenanthrene (PHE), pyrene (PYR), benzo-*a*-pyrene (BAP), anthracene (ANT), benzo-*ghi*-perylene (BGP), benzo-*a*-anthracene (BAA); and PBDEs 47, 99, 100, 153, and 154.

Detailed information on sampling site locations and EMEP sampling and analytical procedures is provided in Table S1 in the ESI.† A map of the sites is provided in Fig. 1. MONET PAS is performed using polyurethane foam (PUF) disk samplers (PUF-

Fig. 1 Locations of the six EMEP/MONET sampling sites across Europe included in this study.

This journal is © The Royal Society of Chemistry 2022

Environ. Sci.: Processes Impacts, 2022, **24**, 898–909 | **899**

PAS); see White *et al.*[3,5] for standard MONET sampling and analytical procedures. Since EMEP sites are operated by different national research laboratories, the sampling, analytical, and data reporting procedures for AAS varied significantly between the six sites (Table S1†). While the sampling and reporting differences can be resolved by further data treatment, a recent global intercomparison suggests that differences in analytical performance between the laboratories may introduce an additional source of uncertainty that limits data comparability.[27] Compared to EMEP, the MONET PAS data and procedures were more consistent between sites since they are all operated by RECETOX. However, there was a change in the MONET sampling procedure at all sites from a 28-d exposure period (2009–2011) to an 84-d exposure period (2011–2018). The temporal sampling regimes of all EMEP AAS and MONET PAS data at all sites are depicted in Fig. S1 in the ESI.†

Data aggregation

Prior to aggregation, all values below the limit of quantification (LOQ) were substituted by $0.5 \times$ LOQ. These substitutions were performed for 5% of OCP, 16% of PCB, 12% of PAH, and 33% of PBDE data from EMEP AAS; and for 3% of OCP, 27% of PCB, 23% of PAH, and 26% of PBDE data from MONET PAS. The LOQs varied depending on the laboratory and monitoring period, ranging from 1×10^{-5} ng m^{-3} for PBDEs to 0.74 ng m^{-3} for PAHs in the AAS measurements and from 3.6×10^{-8} ng d^{-1} for PBDEs to 2.9 ng d^{-1} for PCB 118 in the PAS measurements.

To account for the differences in sampling periods between the sites/networks and to decrease random variability in the data, a quarterly aggregation (91 days) was applied to all EMEP AAS data and all MONET PAS data, separately, within each year (2009–2018). The four quarters of each year were defined as Q1 (January–March), Q2 (April–June), Q3 (July–September), and Q4 (October–December), resulting in 40 concentration values per compound for both the AAS and PAS data over the ten-year monitoring period. The aggregation was carried out as a weighted average of concentrations of the primary samples with different sampling period lengths. The weight of each sample was derived from the number of days in each quarter covered by that sample. For example, if the sample covered only a few days of a specific quarter, its weight was substantially lower compared with a sample spanning over two months within the quarter. The selected 91-d period of the quarters was long enough to cover the 84-d PAS sampling period and several corresponding weekly or monthly AAS sampling periods, while still preserving some measure of seasonal variability in the data (*vs.* annual aggregation).

As previously discussed, some gaps occurred in the AAS and PAS data over the ten-year monitoring period (Fig. S1†). In cases where a gap between two subsequent samples at a site was longer than half of the quarter (>45 days), no data aggregation was performed, and an empty value was assigned to that quarter at that site. Since gaps in sampling varied between networks and sites, only quarters with overlapping aggregated values for both the AAS and PAS data were used for further analysis of field-based R_S (3127 values in total: 655 for OCPs, 1116 for PCBs,

1058 for PAHs, and 298 for PBDEs). Quarterly aggregates for both networks at all sites and all compound groups across the ten-year monitoring period are depicted in Fig. S2.†

Sampling rate computation and analysis

To convert atmospheric SVOC levels measured by MONET PAS (ng d^{-1}) to atmospheric concentrations as measured by EMEP AAS (ng m^{-3}), site- and time-specific R_S values (m^3 d^{-1}) were computed using the two most frequently used models: 'Harner' R_S and 'Herkert' R_S.

The 'Harner' R_S values were computed quarterly with the original GAPS template model[22] using the average temperature over each quarter at each site (eqn (1)):

$$R_S = \frac{V_{\text{air true}}}{\bar{t}} \quad (1)$$

where $V_{\text{air true}}$ is the volume of air sampled over a certain period of time, $\bar{t}$, corrected for the particle sampling efficiency of the sampler (eqn (2)):

$$V_{\text{air true}} = V_{\text{air}} \left(1 - \Phi + \Phi e_{\text{part}}\right) \quad (2)$$

where Φ is the particle-bound fraction of the sampled compound, e_{part} is the efficiency of particle-phase sampling relative to the gas-phase, and V_{air} is the effective air volume sampled by the PAS (eqn (3)):

$$V_{\text{air}} = \overline{K_{\text{PUF-air}}} \times V_{\text{PUF}} \left(1 - \exp\left(-\bar{t} \times \frac{k_{\text{air}}}{\overline{K_{\text{PUF-air}}} \times d_{\text{film}}}\right)\right) \quad (3)$$

where V_{PUF} is the volume of the PUF disk ($V_{\text{PUF}} = 265$ mL for MONET PAS), k_{air} is the air-side mass-transfer coefficient of diffusion ($k_{\text{air}} = 1.1$ mm s^{-1}), d_{film} is the effective thickness of the PUF surface layer ($d_{\text{film}} = 5.67$ mm for MONET PAS), and $\overline{K_{\text{PUF-air}}}$ is the corrected partition coefficient between the air and the PUF disk (eqn (4)):

$$\overline{K_{\text{PUF-air}}} = K_{\text{PUF-air}} \times \rho_{\text{PUF}}$$
$$= \exp(0.6366 \, \log K_{\text{OA}} - 3.1774) \times \rho_{\text{PUF}} \quad (4)$$

where K_{OA} is the temperature-dependent octanol–air partition coefficient of the SVOC and ρ_{PUF} is the density of the PUF disk ($\rho_{\text{PUF}} = 30.0$ kg m^{-3} for MONET PAS).

The 'Herkert' R_S were computed quarterly with the updated GAPS model[23] using hourly temperatures and wind speeds over each quarter at each site (eqn (5)):

$$R_S = A_S \times k_V \quad (5)$$

where A_S is the surface area of the PUF ($A_S = 0.0422543$ m^2 for MONET PAS) and k_V is the mass-transfer coefficient derived from the boundary layer theory equation for laminar flow across a flat plate (eqn (6)):

$$k_V = \gamma \frac{D}{l_{\text{PUF}}} \left(\frac{v_{\text{in}} \times l_{\text{PUF}}}{\mu}\right)^\alpha \left(\frac{\mu}{D}\right)^{\frac{1}{3}} \quad (6)$$

where γ is a dimensionless fitting parameter, D is the molecular diffusivity of the SVOC, l_{PUF} is the diameter of the PUF ($l_{\text{PUF}} =$

900 | *Environ. Sci.: Processes Impacts*, 2022, **24**, 898–909

This journal is © The Royal Society of Chemistry 2022

0.15 m for MONET PAS), μ is the kinematic viscosity, α represents the flow regime as a function of wind speed ($\alpha = 0.5$ for laminar flow), and v_{in} is the internal wind speed within the sampler, which is calculated from the external (site) wind speed, v_{ex}, with a partial linear dependency with two thresholds (1.5 m s^{-1} and 3.0 m s^{-1}) derived from the results of Tuduri et al.[15] (eqn (7)):

$$v_{in} = \begin{cases} 0.1608\ v_{ex}, & v_{ex} < 1.5 \text{ m s}^{-1} \\ 0.2385\ v_{ex}, & 1.5 \text{ m s}^{-1} < v_{ex} < 3.0 \text{ m s}^{-1} \\ 0.2703\ v_{ex}, & v_{ex} > 3.0 \text{ m s}^{-1} \end{cases} \quad (7)$$

Detailed information on the derivation of these equations and the use of these two models is provided elsewhere;[8,12,14,21,23,28] see Table S2† for a list of model input parameters used for MONET PAS. Since consistent meteorological measurements over the monitoring period were not available at every site, all meteorological parameters necessary for sampling rate computations were generated hourly over the entire monitoring period (2009–2018) using the NASA MERRA-2 model,[29] as previously described.[3,8,23] To assess differences between R_S values generated by these models and real monitored data, a third set of R_S values was calculated ('field' R_S) based on the ratios of PAS:AAS aggregated values corresponding to the same sampling quarter.

It is important to note that PAS concentrations were calculated twice using both models. The initial calculations were based on the default e_{part} value of 100% typically used for GAPS PAS. It has previously been observed that the e_{part} value for MONET PAS is substantially lower than 100% due to differences in sampler design between MONET and GAPS,[24,30] but the range of values reported is large with no consensus. However, the unrealistically high R_S values modelled in the initial run made it possible to calibrate a MONET PAS-specific e_{part} value so that adjusted PAS concentrations could be calculated a second time with both models.

The statistical significance of differences between the three R_S sets for all individual compounds, sites, and quarters was evaluated with the Mann–Whitney U test[31] and the Kruskal–Wallis test.[32] Compared to the modelled R_S, the field R_S spanned several orders of magnitude, including some extremely high and low values that may have been caused by contamination during sample handling and transport, or errors in compound analysis and data treatment. To prevent the results of this study from being affected by such extreme values, lower and upper thresholds (L, U) were set for each site/compound subset of R_S as $L, U = \exp\{\widehat{\log(X)} \mp IQR(\log(X))\}$ where X is the R_S subset, $\widehat{\log(X)}$ is the median over the log-transformed R_S values in the subset, and $IQR(\log(X))$ is the interquartile range of the log-transformed R_S values in the subset. In total, 3% of the field R_S values exceeded these thresholds and were removed from the dataset as outliers. This correction assumes that the R_S are approximately log-normally distributed, as confirmed in Fig. S3.†

Results & discussion

Concentrations and sampling rates

Atmospheric MONET PAS concentrations initially calculated from both models with an e_{part} value of 100% were generally higher than the corresponding EMEP AAS concentrations. The magnitude of this difference varied greatly depending on model-, site-, and compound-specific factors. AAS and PAS (Harner- and Herkert-modelled) concentrations over the 10-year monitoring period are presented for eight selected SVOCs (two from each compound class) in Fig. 2; see Fig. S4† for all remaining SVOCs. Of the 127 site/compound comparisons included in this study, only 22% of the Harner-modelled PAS concentrations, and 11% of the Herkert-modelled PAS concentrations, were not significantly different from their corresponding AAS concentrations ($p > 0.05$). However, it is well established that PAS provides long-term integrations rather than concentrations identical to those from AAS; the agreement is generally deemed to be strong if PAS concentrations are within a factor of 2–3 of AAS concentrations.[10,33] According to this more lenient criterion, 79% of the Harner-modelled median PAS concentrations are within a factor of 3 of the corresponding AAS concentrations (Table S3†). In comparison, only 60% of the Herkert-modelled median PAS concentrations are within a factor of 3 of the corresponding AAS concentrations due to significantly higher concentrations for the majority of SVOCs at both Birkenes and Pallas when compared to the Harner-modelled concentrations. This discrepancy was unexpected, as previous studies have found negligible differences in the output concentrations between the two models for most sites/compounds,[8,34] despite their different input parameters. Similar negligible differences were observed in this study at the other four sites, with median PAS concentrations from the two models falling within a factor of 1.5 of each other for all SVOCs at Košetice, Råö, Stórhöfði, and Zeppelin. However, as mentioned above, Herkert-modelled concentrations are 2.8–4.8 times higher than the corresponding Harner-modelled concentrations for all SVOCs at Birkenes, and 2.0–4.8 times higher at Pallas, suggesting some site-specific influences at these two sites on input parameters for the Herkert model that are not incorporated in the Harner model, such as wind speed. The other major site-specific result was at Stórhöfði, where both models yielded significantly higher PAS concentrations for all SVOCs except the lowest-molecular-weight PCBs (28, 52, 101) and PBDEs (47, 99, 100); for the remaining SVOCs, Harner-modelled median PAS concentrations are 9–44 times higher than the corresponding AAS concentrations, and Herkert-modelled concentrations are 8–37 times higher.

The Harner R_S values are relatively constant across all site/compound combinations, with median values spanning 3.3–4.4 m^3 d^{-1}. The Herkert R_S values are similar to these values at Košetice, Råö, Stórhöfði, and Zeppelin, but with slightly more variability in the median values, ranging from 2.3 to 5.7 m^3 d^{-1} (Table S4†). In contrast, the Herkert R_S values are substantially lower at Birkenes and Pallas compared to the other sites, with

This journal is © The Royal Society of Chemistry 2022

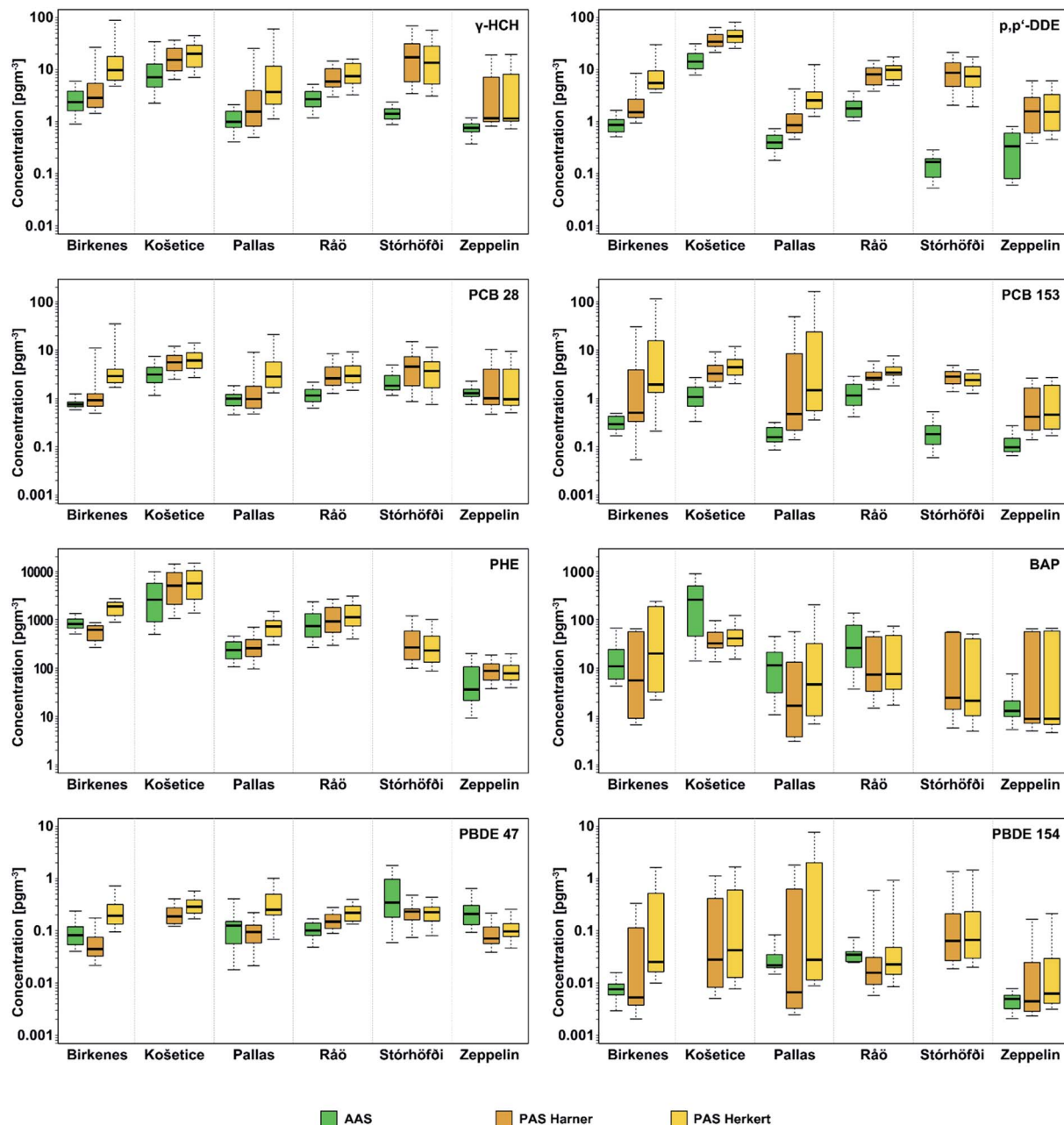*Environ. Sci.: Processes Impacts*, 2022, **24**, 898–909 | **901**

Fig. 2 Boxplots of SVOC concentrations in air (two selected representatives in each compound class) from EMEP active air sampling (AAS) and MONET passive air sampling (PAS) calculated by the 'Harner' and 'Herkert' models ($e_{part} = 100\%$). Boxplots represent ten years of overlapping monitoring data (2009–2018). Thick black lines represent medians, boxes span from 25th to 75th percentiles, and whiskers represent the 5th and 95th percentiles. See Fig. S4† for all other SVOCs included in this study.

median values ranging 1.0–1.7 m³ d⁻¹ (Table S4†), resulting in the significant difference between the Harner- and Herkert-modelled concentrations observed at these two sites (Fig. 2). Conversely, the high modelled concentrations by both models at Stórhöfði correspond to extremely high field R_S values at this site, with median values ranging 12–66 m³ d⁻¹ for PCBs and 45–280 m³ d⁻¹ for OCPs (Table S4†). Aside from Stórhöfði, the field R_S still varied to a significantly greater extent across all other site/compound combinations compared to the Harner and

Herkert R_S, with median field R_S ranging two orders of magnitude from 0.3–33 m³ d⁻¹ (Fig. 3; see Fig. S5† for all SVOCs).

These differences in field R_S between sites are affected by variations in meteorological conditions, frequency and duration of AAS and PAS sampling, analytical procedures and performance (AAS data are from four different laboratories; Table S1†),[27] and random variation associated with individual values.[35] Differences caused by meteorological factors are partially accounted for in the mathematical models for kinetic

902 | Environ. Sci.: Processes Impacts, 2022, **24**, 898–909

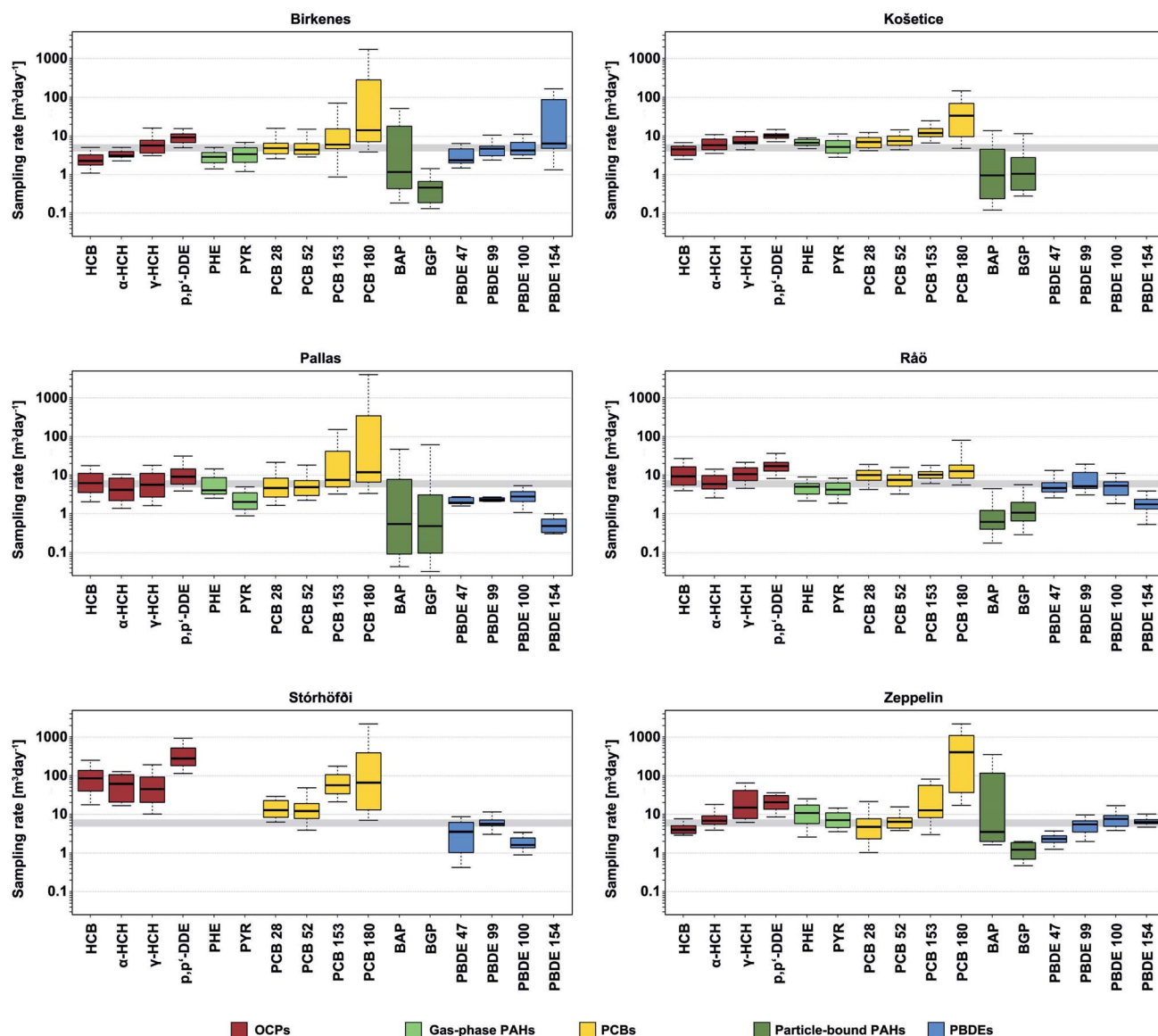This journal is © The Royal Society of Chemistry 2022

Fig. 3 Boxplots of field sampling rates derived from quarterly-aggregated EMEP AAS and MONET PAS SVOC data measured at six stations during the period 2009–2018 ($n = 8$–39; Fig. S2†). Four selected representatives within each SVOC group are presented and distinguished by colour: OCPs (red), PAHs (light and dark green representing predominantly gas-phase and particle-bound PAHs, respectively), PCBs (yellow), and PBDEs (blue). SVOC groups and individual compounds are ordered by increasing K_{OA} from left to right. Thick black lines represent medians, boxes range from 25th to 75th percentiles, and whiskers represent the 5th and 95th percentiles. Narrow grey shaded areas represent the range of R_S often used for PAS (4–6 m³ d⁻¹).

sampling[22,23] and random variation in both AAS and PAS data may be reduced by repeated sampling over longer periods of time.[4,9] In addition, the inherent chemical properties of individual SVOCs also affect their R_S. In particular, the octanol-air partition coefficient (K_{OA}) of SVOCs plays a key role in their uptake by passive samplers,[10,14] and accurately describes many of the compound-specific differences in field R_S observed in this study. For example, field R_S increased with increasing log K_{OA} for the SVOCs predominantly (>95%) in the gas phase (log K_{OA} < 8.8),[4] *e.g.*, α-HCH, γ-HCH, HCB, PCB 28, PCB 52, FLU, PHE, ANT, with PAS uptake of these compounds primarily controlled by absorption dynamics.[22,28] In contrast, field R_S decreased for

the transition group of SVOCs (8.8 < log K_{OA} < 11.3) due to a shift from predominantly in the gas-phase to the particle-bound phase. Finally, for the SVOCs predominantly (>95%) in the particle phase (log K_{OA} > 11.3), *e.g.*, BAP, BGP, PBDE 153, PBDE 154, the field R_S were approximately one order of magnitude lower than for the gas-phase SVOCs, as previously observed for MONET PAS[8,10] due to low particle sampling efficiency.[4,30]

Influence of particle sampling efficiency

It is important to note that the Harner and Herkert models were both calibrated and developed based on GAPS passive samplers

This journal is © The Royal Society of Chemistry 2022

Environ. Sci.: Processes Impacts, 2022, **24**, 898–909 | **903**

and initially run here on the default assumption that they have an atmospheric particle sampling efficiency (e_{part}) of 100%.[22,23] Previous studies of gas-particle partitioning have observed that MONET passive samplers have a much lower e_{part}, but the values range considerably, from the frequently used estimate of 10% (ref. 16) to as high as 54%,[30] so it was deemed necessary to derive a MONET-specific e_{part} value to accurately model PAS-derived concentrations. Previous MONET studies have reported R_S values of primarily particle-bound SVOCs such as higher-molecular-weight PAHs and PBDEs approximately one order of magnitude lower than those of predominantly gas-phase SVOCs.[4,8,10,16] The same effect is apparent in the present study for more than 70% of the particle-bound SVOC (log K_{OA} > 11.3), with a median ratio of field-to-modelled R_S values of 0.32 for the Harner R_S and 0.52 for the Herkert R_S values. This indicates that the modelled R_S values for these compounds are overestimated if not adjusted for the lower e_{part} (see Table 1 for individual sites). In contrast, the median ratio between field- and modelled-R_S values of the gas-phase SVOCs (log K_{OA} < 8.8) is 1.53 for the Harner R_S and 2.33 for the Herkert R_S.

Over all sites, the ratios of field-to-modelled R_S values for the particle-phase SVOCs are lower by a factor of 0.18 than the ratios for the gas-phase SVOCs (16% for Harner R_S and 19% for Herkert R_S). This suggests that, for the particle-bound SVOCs, the modelled R_S values are overestimated by a factor of approximately five (1/0.18). This value of 18% was therefore used as an empirical estimate of the MONET-specific PAS particle sampling efficiency; it is significantly lower than the default 100% value, but consistent with the 10% estimate[16] typically used for MONET PAS. All Harner- and Herkert-modelled concentrations and R_S values were therefore adjusted and recalculated with e_{part} = 18% rather than the default of 100%, following the same method as Bohlin-Nizzetto et al.,[8] and these adjusted R_S values were used for further analysis. This adjustment had negligible effects on the modelled concentrations of the gas-phase SVOCs but led to an increase in the modelled concentrations of the particle-phase SVOCs (Table 1). As a result, the differences between PAS and AAS concentrations became more similar for gas-phase and particle-bound SVOCs at most sites (Fig. 4), but some site-specific discrepancies persisted and were attributed to local meteorological differences, particularly wind speed.

Influence of wind speed

The major difference between the Harner and Herkert models is how the R_S values are affected by local meteorology. The Harner model simply incorporates average site temperatures over the deployment period;[22] the Herkert model incorporates more detailed meteorological parameters at a much greater time resolution, including hourly wind speeds.[23] While the Harner model has proven to be reliable for calculating concentrations of SVOCs from PAS at most GAPS sampling sites around the world, elevated R_S values have been observed at some extremely windy sites.[36,37] The influence of wind speed on R_S has been thoroughly explored by Tuduri et al.,[15] who found that an external wind speed of approximately 4 m s^{-1} represents the threshold corresponding to a change in internal airflow within the sampler from laminar to turbulent for the PAS used by both MONET and GAPS.[18] For wind speeds from 0–4 m s^{-1}, R_S (for PCBs) gradually increases from approximately 4.5 to 15 m^3 d^{-1}; however, R_S sharply increases with increasing wind speeds above 4 m s^{-1}, up to ~40 m^3 d^{-1} at 7.5 m s^{-1}.[15] This effect provides a likely explanation for the significantly elevated field-R_S values, and lower values of the modelled R_S, observed here primarily at Stórhöfði. Not only is Stórhöfði the windiest meteorological station in Europe,[38] but it was also the only site included in this study with a median wind speed over the entire monitoring period greater than 4 m s^{-1} (5.2 m s^{-1}), with 66% of the hourly wind speeds exceeding this threshold (Table 2) and some even exceeding 20 m s^{-1} (Fig. S7†). Conversely, median wind speeds at Košetice, Råö, and Zeppelin were 2.7–3.5 m s^{-1} (with only 20–42% of hourly wind speeds above 4 m s^{-1}), corresponding to good agreement between field and modelled R_S, as previously discussed.

The Herkert model was designed as an improvement to the original Harner model by incorporating the results of Tuduri et al.[15] to account for the influence of wind speed on R_S at particularly windy sites. However, the R_S values from the Herkert model are still significantly lower than the field R_S (Table 2). The dependency of R_S on external wind speed (v_{ex}) within the Herkert model (i.e., $R_S \sim f(v_{ex})$) is not continuous but rather defined for three wind speed ranges (<1.5 m s^{-1}, 1.5–3.0 m s^{-1}, >3.0 m s^{-1}) as shown in eqn (7). While the magnitude of this dependency varies between the three ranges, the underlying

Table 1 Median ratios of field-based sampling rates to Harner- and Herkert-modelled sampling rates. Medians were computed over the 10 year monitoring period (2009–2018) for gas-phase SVOCs (log K_{OA} < 8.8) and particle-phase SVOCs (log K_{OA} > 11.3) with MONET PAS particle sampling efficiencies of both 100% and 18%

	Birkenes		Košetice		Pallas		Råö		Stórhöfði		Zeppelin	
Particle sampling efficiency (e_{part})	100%	18%	100%	18%	100%	18%	100%	18%	100%	18%	100%	18%
Gas phase SVOCs (log K_{OA} < 8.8)												
Field R_S/Harner R_S	0.9	0.9	1.6	1.6	1.0	1.1	1.8	1.8	11.3	11.4	1.7	1.7
Field R_S/Herkert R_S	2.8	2.8	1.9	1.9	2.6	2.8	2.0	2.0	9.1	9.2	1.7	1.7
Particle phase SVOCs (log K_{OA} > 11.3)												
Field R_S/Harner R_S	0.6	2.7	0.2	0.7	0.2	0.8	0.3	1.1	—	—	0.8	2.7
Field R_S/Herkert R_S	2.6	9.7	0.2	0.8	0.5	2.4	0.3	1.5	—	—	0.8	2.8

904 | Environ. Sci.: Processes Impacts, 2022, **24**, 898–909
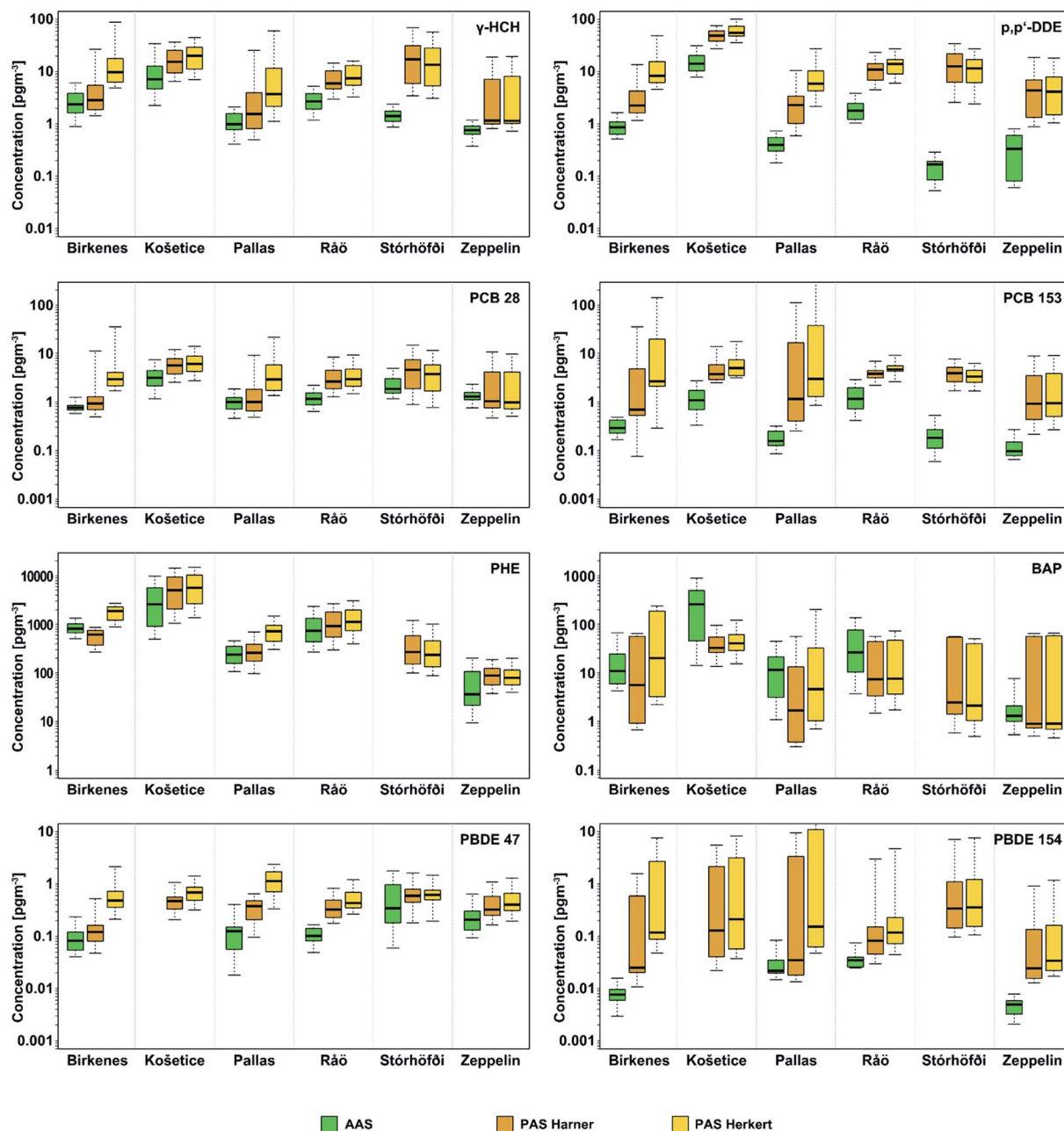
This journal is © The Royal Society of Chemistry 2022

Fig. 4 Boxplots of SVOC concentrations in air from EMEP active air sampling (AAS) and MONET passive air sampling (PAS) calculated by the adjusted 'Harner' and 'Herkert' models (e_{part} = 18%). Boxplots represent ten years of overlapping monitoring data (2009–2018). Thick black lines represent medians, boxes span from 25th to 75th percentiles, and whiskers represent the 5th and 95th percentiles. See Fig. S6† for all other SVOCs included in this study.

relationship remains linear in the square root of v_{ex} ($R_S \sim f(v_{ex}{}^{\alpha})$); where $\alpha = 0.5$ for laminar flow under all conditions).[21] Yet studies have shown that when turbulent airflow conditions exist within the sampler (e.g., when the external wind speed exceeds 4.0 m s^{-1}), the dependency of R_S on v_{ex} is stronger, ranging from sub-linear ($\alpha = 0.63$),[34] to linear ($\alpha = 1$),[16,19] or greater than linear ($\alpha > 1$).[15,20,39,40] As a result, the constant square-root shape of the dependency, regardless of extremely high wind speeds, leads to an underestimation of modelled R_S over periods of strong wind.

The discrepancy between the modelled Harner R_S and Herkert R_S at Birkenes and Pallas is the other major site-specific result identified in this study. As previously discussed, Herkert R_S values at these two sites were significantly lower than both the field R_S and the Harner R_S, suggesting a site- and model-specific effect such as wind speed as observed at Stórhöfði. However, the hourly wind speeds at these two sites were substantially lower than at the other four sites, with medians of 0.5–0.6 m s^{-1} and 0% exceeding the 4 m s^{-1} threshold (Table 2 and Fig. S7†). This indicates that the Herkert model also underestimates R_S at sites

This journal is © The Royal Society of Chemistry 2022

Environ. Sci.: Processes Impacts, 2022, 24, 898–909 | 905

Table 2 Median ratios between the field-derived and modelled R_S values ($e_{part} = 18\%$) and their comparison with site-specific wind-speed parameters. Medians were computed from all quarterly aggregates for all compounds over the whole monitoring period

	Birkenes	Košetice	Pallas	Råö	Stórhöfði	Zeppelin
Ratios of median sampling rates						
Field R_S/Harner R_S	0.9	1.6	1.0	1.5	7.6	1.7
Field R_S/Herkert R_S	3.2	2.0	2.6	1.8	7.0	1.8
Hourly wind speed data						
Median wind speed (m s^{-1})	0.5	2.7	0.6	2.8	5.2	3.5
Wind speeds >4 m s^{-1} (%)	0	23	0	20	66	42
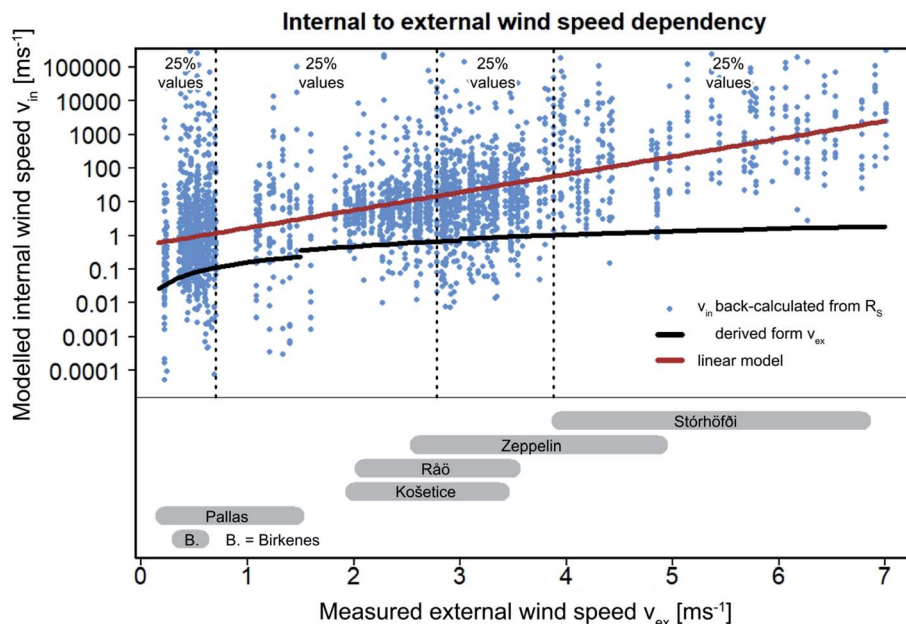
Fig. 5 Relationship between internal wind speed, v_{in}, and external wind speed, v_{ex}, for theoretical values of v_{in} back-calculated from field R_S (blue dots) and the stepwise linear dependency (eqn (7)) of v_{in} on v_{ex} used within the Herkert model (black line). The red line was estimated by a linear model on log-transformed v_{in} values and represents the relationship between v_{in} and v_{ex} as the best fit of the field data. Wind speed ranges (5th to 95th percentile of median wind speeds over the sampling period) for the six sites are depicted as horizontal grey bars.

with very low wind speeds. Schuster *et al.*[34] suggest this may be an artifact of the MERRA meteorological model underestimating wind speeds at sites where presence of a forest cover may have been incorrectly assumed.

By applying the square-root dependency between the mass transfer coefficient (k_V) and the internal wind speed (v_{in}) within the Herkert model ($\alpha = 0.5$, eqn (6)), we derived a set of theoretical v_{in} values back-calculated from all of the field R_S derived in this study (blue dots in Fig. 5). A substantial number of these back-calculated v_{in} values are extremely high (Fig. 5), providing further evidence that the square-root dependency of $\alpha = 0.5$ is unrealistic for high external wind speeds (v_{ex}). We then compared the back-calculated v_{in} values with modelled values of v_{in} derived from the external wind speeds within the model by eqn (7) (black line in Fig. 5). The discrepancy between these two sets of data is presented in Fig. 5 and indicates an underestimation of R_S by the Herkert model by approximately a factor of 2 at Råö, Košetice and Pallas, and increasing in magnitude with both decreasing wind speed (factor of 3 at Birkenes) and

increasing wind speed (up to several orders of magnitude at Stórhöfði).

Overall, the Harner model works well for the majority of sites, with some well-established uncertainties due to the exclusion of meteorological parameters other than temperature, but substantially underestimates R_S if wind speed exceeds 4 m s^{-1}. Conversely, the Herkert model is well designed for incorporating the influence of wind speed, but the brief calibration conducted in this study on a ten-year-long data series from sites with different meteorological conditions indicates that the dependency of the mass transfer coefficient, k_V, on external wind speed, v_{ex} may be too shallow, leading to an underestimation of R_S at sites with particularly low or high wind speeds.

Conclusions

Long-term atmospheric data from the major global semivolatile organic compound monitoring networks using active or passive air sampling have been shown to be internally consistent and to

906 | *Environ. Sci.: Processes Impacts*, 2022, **24**, 898–909

This journal is © The Royal Society of Chemistry 2022
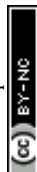
provide similar temporal trends, even when concentration units are not directly comparable. However, data harmonization between active EMEP air sampling and passive MONET air sampling – the two largest atmospheric SVOC monitoring networks in Europe – is still essential for more comprehensive evaluations of the effectiveness of both regional and global regulatory measures on these chemicals, as well as assessments of their impacts on environmental and human health across the continent. After 10 years of continuous parallel monitoring, results of this study indicate that there is good agreement between the long-term atmospheric SVOC concentrations measured by the two networks and methods, with nearly 80% of the median MONET PAS concentrations falling within a factor of 3 of their corresponding EMEP AAS concentrations. However, we have identified several cases where the agreement was poor, so any potential pooling of data must consider these cases and their conditions. For compound-specific considerations, the sampler-specific particle sampling efficiency of any passive sampler design should be well understood and accounted for in models for calculating R_S. For site-specific considerations, modelled PAS concentrations are substantially overestimated compared to AAS at sites where the wind speed consistently exceeds 4 m s^{-1}. We have provided a potential adjustment to the Herkert model to address this issue by increasing the power of the dependency (α) between the mass-transfer coefficient (k_V) and the site wind speed (v_{ex}) to account for a possible transition from laminar to turbulent airflow within passive samplers. However, such an adjustment will require more in-depth model calibration and development beyond the scope of this study. Until the Herkert model can more accurately estimate atmospheric concentrations at high wind speeds, PAS concentrations from windy sites (above 4 m s^{-1}) should be excluded from any comparisons to AAS concentrations. It should also be noted that even in cases where the long-term agreement was strong, substantial variability can be observed in comparisons of individual samples or shorter time periods, which may limit the potential for pooling short-term AAS and PAS data. Nonetheless, the strong agreement observed between the majority of AAS and PAS concentrations for most SVOCs and sites provides support for the harmonization and pooling of long-term EMEP and MONET concentration data as long as the compound- and site-specific recommendations are followed.

Conflicts of interest

There are no conflicts to declare.

Acknowledgements

References

1 K. Tørseth, W. Aas, K. Breivik, a. M. Fjeraa, M. Fiebig, A.-G. Hjellbrekke, C. Lund Myhre, S. Solberg and K. E. Yttri, Introduction to the European Monitoring and Evaluation Programme (EMEP) and Observed Atmospheric Composition Change during 1972–2009, *Atmos. Chem. Phys.*, 2012, **12**(12), 5447–5481, DOI: **10.5194/acp-12-5447-2012**.

2 P. Pribylova, R. Kares, J. Boruvkova, P. Cupr, R. Prokes, J. Kohoutek, I. Holoubek and J. Klanova, Levels of Persistent Organic Pollutants and Polycyclic Aromatic Hydrocarbons in Ambient Air of Central and Eastern Europe, *Atmos. Pollut. Res.*, 2012, **3**(4), 494–505, DOI: **10.5094/apr.2012.057**.

3 K. B. White, J. Kalina, M. Scheringer, P. Přibylová, P. Kukučka, J. Kohoutek, R. Prokeš and J. Klánová, Temporal Trends of Persistent Organic Pollutants across Africa after a Decade of MONET Passive Air Sampling, *Environ. Sci. Technol.*, 2021, **55**, 9413–9424, DOI: **10.1021/acs.est.0c03575**.

4 J. Kalina, M. Scheringer, J. Borůvková, P. Kukučka, P. Přibylová, P. Bohlin-Nizzetto and J. Klánová, Passive Air Samplers As a Tool for Assessing Long-Term Trends in Atmospheric Concentrations of Semivolatile Organic Compounds, *Environ. Sci. Technol.*, 2017, **51**(12), 7047–7054, DOI: **10.1021/acs.est.7b02319**.

5 K. B. White, O. Sáňka, L. Melymuk, P. Přibylová and J. Klánová, Application of Land Use Regression Modelling to Describe Atmospheric Levels of Semivolatile Organic Compounds on a National Scale, *Sci. Total Environ.*, 2021, **793**, 148520, DOI: **10.1016/j.scitotenv.2021.148520**.

6 J. Kalina, M. Scheringer, J. Borůvková, P. Kukučka, P. Přibylová, O. Sáňka, L. Melymuk, M. Váňa and J. Klánová, Characterizing Spatial Diversity of Passive Sampling Sites for Measuring Levels and Trends of Semivolatile Organic Chemicals, *Environ. Sci. Technol.*, 2018, **52**, 10599–10608, DOI: **10.1021/acs.est.8b03414**.

This journal is © The Royal Society of Chemistry 2022

Environ. Sci.: Processes Impacts, 2022, **24**, 898–909 | **907**

7 F. Wania and C. Shunthirasingham, Passive Air Sampling for Semi-Volatile Organic Chemicals, *Environ. Sci.: Processes Impacts*, 2020, **22**(10), 1925–2002, DOI: **10.1039/D0EM00194E**.

8 P. Bohlin-Nizzetto, L. Melymuk, K. B. White, J. Kalina, V. O. Madadi, S. Adu-Kumi, R. Prokeš, P. Přibylová and J. Klánová, Field- and Model-Based Calibration of Polyurethane Foam Passive Air Samplers in Different Climate Regions Highlights Differences in Sampler Uptake Performance, *Atmos. Environ.*, 2020, **238**, 117742, DOI: **10.1016/j.atmosenv.2020.117742**.

9 J. Kalina, K. B. White, M. Scheringer, P. Přibylová, P. Kukučka, O. Audy and J. Klánová, Comparability of Long-Term Temporal Trends of POPs from Co-Located Active and Passive Air Monitoring Networks in Europe, *Environ. Sci.: Processes Impacts*, 2019, **21**(7), 1132–1142, DOI: **10.1039/c9em00136k**.

10 E. Holt, P. Bohlin-Nizzetto, J. Borůvková, T. Harner, J. Kalina, L. Melymuk and J. Klánová, Using Long-Term Air Monitoring of Semi-Volatile Organic Compounds to Evaluate the Uncertainty in Polyurethane-Disk Passive Sampler-Derived Air Concentrations, *Environ. Pollut.*, 2017, **220**, 1100–1111, DOI: **10.1016/j.envpol.2016.11.030**.

11 L. Melymuk, P. Bohlin, O. Sáňka, K. Pozo and J. Klánová, Current Challenges in Air Sampling of Semivolatile Organic Contaminants: Sampling Artifacts and Their Influence on Data Comparability, *Environ. Sci. Technol.*, 2014, **48**(24), 14077–14091, DOI: **10.1021/es502164r**.

12 N. T. Petrich, S. N. Spak, G. R. Carmichael, D. Hu, A. Martinez and K. C. Hornbuckle, Simulating and Explaining Passive Air Sampling Rates for Semivolatile Compounds on Polyurethane Foam Passive Samplers, *Environ. Sci. Technol.*, 2013, **47**(15), 8591–8598, DOI: **10.1021/es401532q**.

13 C. Moeckel, T. Harner, L. Nizzetto, B. Strandberg, A. Lindroth and K. C. Jones, Use of Depuration Compounds in Passive Air Samplers: Results from Active Sampling-Supported Field Deployment, Potential Uses, and Recommendations, *Environ. Sci. Technol.*, 2009, **43**(9), 3227–3232, DOI: **10.1021/es802897x**.

14 M. Shoeib and T. Harner, Using Measured Octanol-Air Partition Coefficients to Explain Environmental Partitioning of Organochlorine Pesticides, *Environ. Toxicol. Chem.*, 2002, **21**(5), 984–990, DOI: **10.1002/etc.5620210513**.

15 L. Tuduri, T. Harner and H. Hung, Polyurethane Foam (PUF) Disks Passive Air Samplers: Wind Effect on Sampling Rates, *Environ. Pollut.*, 2006, **144**(2), 377–383, DOI: **10.1016/J.ENVPOL.2005.12.047**.

16 J. Klánová, P. Čupr, J. Kohoutek and T. Harner, Assessing the Influence of Meteorological Parameters on the Performance of Polyurethane Foam-Based Passive Air Samplers, *Environ. Sci. Technol.*, 2008, **42**(2), 550–555, DOI: **10.1021/es072098o**.

17 C. Chaemfa, E. Wild, B. Davison, J. L. Barber and K. C. Jones, A Study of Aerosol Entrapment and the Influence of Wind Speed, Chamber Design and Foam Density on Polyurethane Foam Passive Air Samplers Used for

Persistent Organic Pollutants, *J. Environ. Monit.*, 2009, **11**(6), 1135–1139, DOI: **10.1039/b823016a**.

18 J. Thomas, T. M. Holsen and S. Dhaniyala, Computational Fluid Dynamic Modeling of Two Passive Samplers, *Environ. Pollut.*, 2006, **144**(2), 384–392, DOI: **10.1016/j.envpol.2005.12.042**.

19 A. A. May, P. Ashman, J. Huang, S. Dhaniyala and T. M. Holsen, Evaluation of the Polyurethane Foam (PUF) Disk Passive Air Sampler: Computational Modeling and Experimental Measurements, *Atmos. Environ.*, 2011, **45**(26), 4354–4359, DOI: **10.1016/j.atmosenv.2011.05.052**.

20 P. C. Tromp, H. Beeltje, J. O. Okeme, R. Vermeulen, A. Pronk and M. L. Diamond, Calibration of Polydimethylsiloxane and Polyurethane Foam Passive Air Samplers for Measuring Semi Volatile Organic Compounds Using a Novel Exposure Chamber Design, *Chemosphere*, 2019, **227**, 435–443, DOI: **10.1016/j.chemosphere.2019.04.043**.

21 N. J. Herkert, A. Martinez and K. C. Hornbuckle, A Model Using Local Weather Data to Determine the Effective Sampling Volume for PCB Congeners Collected on Passive Air Samplers, *Environ. Sci. Technol.*, 2016, **50**(13), 6690–6697, DOI: **10.1021/acs.est.6b00319**.

22 T. Harner, *2017_v1_5_Template for Calculating Effective Air Sample Volumes for PUF and SIP Disk Samplers_Sept_15*, 2017.

23 N. J. Herkert, S. N. Spak, A. Smith, J. K. Schuster, T. Harner, A. Martinez and K. C. Hornbuckle, Calibration and Evaluation of PUF-PAS Sampling Rates across the Global Atmospheric Passive Sampling (GAPS) Network, *Environ. Sci.: Processes Impacts*, 2018, **20**(1), 210–219, DOI: **10.1039/c7em00360a**.

24 J. Klánová, J. Kohoutek, L. Hamplová, P. Urbanová and I. Holoubek, Passive Air Sampler as a Tool for Long-Term Air Pollution Monitoring: Part 1. Performance Assessment for Seasonal and Spatial Variations, *Environ. Pollut.*, 2006, **144**(2), 393–405, DOI: **10.1016/j.envpol.2005.12.048**.

25 P. Čupr, J. Klánová, T. Bartoš, Z. Flegrová, J. Kohoutek and I. Holoubek, Passive Air Sampler as a Tool for Long-Term Air Pollution Monitoring: Part 2. Air Genotoxic Potency Screening Assessment, *Environ. Pollut.*, 2006, **144**(2), 406–413, DOI: **10.1016/j.envpol.2005.12.045**.

26 L. Melymuk, P. Bohlin-Nizzetto, R. Prokeš, P. Kukučka and J. Klánová, Sampling Artifacts in Active Air Sampling of Semivolatile Organic Contaminants: Comparing Theoretical and Measured Artifacts and Evaluating Implications for Monitoring Networks, *Environ. Pollut.*, 2016, **217**, 97–106, DOI: **10.1016/j.envpol.2015.12.015**.

27 L. Melymuk, P. B. Nizzetto, T. Harner, K. B. White, X. Wang, M. Y. Tominaga, J. He, J. Li, J. Ma, W.-L. Ma, B. H. Aristizábal, A. Dryer, B. Jimenéz, J. Muñoz-Arnanz, M. Odabasi, Y. Dumanoglu, B. Yaman, C. Graf, A. Sweetman and J. Klánová, Global Intercomparison of Polyurethane Foam Passive Air Samplers Evaluating Sources of Variability in SVOC Measurements, *Environ. Sci. Policy*, 2021, **125**, 1–9, DOI: **10.1016/j.envsci.2021.08.003**.

28 M. Shoeib and T. Harner, Characterization and Comparison of Three Passive Air Samplers for Persistent Organic

908 | *Environ. Sci.: Processes Impacts*, 2022, **24**, 898–909

This journal is © The Royal Society of Chemistry 2022

Pollutants, *Environ. Sci. Technol.*, 2002, **36**(19), 4142–4151, DOI: **10.1021/es020635t**.

29 R. Gelaro, W. McCarty, M. J. Suárez, R. Todling, A. Molod, L. Takacs, C. A. Randles, A. Darmenov, M. G. Bosilovich, R. Reichle, K. Wargan, L. Coy, R. Cullather, C. Draper, S. Akella, V. Buchard, A. Conaty, A. M. da Silva, W. Gu, G.-K. Kim, R. Koster, R. Lucchesi, D. Merkova, J. E. Nielsen, G. Partyka, S. Pawson, W. Putman, M. Rienecker, S. D. Schubert, M. Sienkiewicz and B. Zhao, The Modern-Era Retrospective Analysis for Research and Applications, Version 2 (MERRA-2), *J. Clim.*, 2017, **30**(14), 5419–5454, DOI: **10.1175/JCLI-D-16-0758.1**.

30 M. Z. Markovic, S. Prokop, R. M. Staebler, J. Liggio and T. Harner, Evaluation of the Particle Infiltration Efficiency of Three Passive Samplers and the PS-1 Active Air Sampler, *Atmos. Environ.*, 2015, **112**, 289–293, DOI: **10.1016/j.atmosenv.2015.04.051**.

31 H. B. Mann and D. R. Whitney, On a Test of Whether One of Two Random Variables Is Stochastically Larger than the Other, *Ann. Math. Stat.*, 1947, **18**(1), 50–60, DOI: **10.1214/aoms/1177730491**.

32 W. H. Kruskal and W. A. Wallis, Use of Ranks in One-Criterion Variance Analysis, *J. Am. Stat. Assoc.*, 1952, **47**(260), 583, DOI: **10.2307/2280779**.

33 T. Harner, M. Bartkow, I. Holoubek, J. Klanova, F. Wania, R. Gioia, C. Moeckel, A. J. Sweetman and K. C. Jones, Passive Air Sampling for Persistent Organic Pollutants: Introductory Remarks to the Special Issue, *Environ. Pollut.*, 2006, **144**(2), 361–364, DOI: **10.1016/j.envpol.2005.12.044**.

34 J. K. Schuster, T. Harner, A. Eng, C. Rauert, K. Su, K. C. Hornbuckle and C. W. Johnson, Tracking POPs in Global Air from the First 10 Years of the GAPS Network

(2005 to 2014), *Environ. Sci. Technol.*, 2021, **55**, 9479–9488, DOI: **10.1021/acs.est.1c01705**.

35 Y. Li and F. Wania, Partitioning between Polyurethane Foam and the Gas Phase: Data Compilation, Uncertainty Estimation and Implications for Air Sampling, *Environ. Sci.: Processes Impacts*, 2021, **23**(5), 723–734, DOI: **10.1039/d1em00036e**.

36 K. Pozo, T. Harner, F. Wania, D. C. G. Muir, K. C. Jones and L. A. Barrie, Toward a Global Network for Persistent Organic Pollutants in Air: Results from the GAPS Study, *Environ. Sci. Technol.*, 2006, **40**(16), 4867–4873, DOI: **10.1021/es060447t**.

37 K. Pozo, T. Harner, S. C. Lee, F. Wania, D. C. G. Muir and K. C. Jones, Seasonally Resolved Concentrations of Persistent Organic Pollutants in the Global Atmosphere from the First Year of the GAPS Study, *Environ. Sci. Technol.*, 2009, **43**(3), 796–803, DOI: **10.1021/es802106a**.

38 P. Dagsson-Waldhauserova, O. Arnalds and H. Olafsson, Long-Term Variability of Dust Events in Iceland (1949–2011), *Atmos. Chem. Phys.*, 2014, **14**(24), 13411–13422, DOI: **10.5194/acp-14-13411-2014**.

39 L. Melymuk, M. Robson, P. A. Helm and M. L. Diamond, Evaluation of Passive Air Sampler Calibrations: Selection of Sampling Rates and Implications for the Measurement of Persistent Organic Pollutants in Air, *Atmos. Environ.*, 2011, **45**(10), 1867–1875, DOI: **10.1016/j.atmosenv.2011.01.011**.

40 C. Moeckel, T. Harner, L. Nizzetto, B. Strandberg, A. Lindroth and K. C. Jones, Use of Depuration Compounds in Passive Air Samplers: Results from Active Sampling-Supported Field Deployment, Potential Uses, and Recommendations, *Environ. Sci. Technol.*, 2009, **43**(9), 3227–3232, DOI: **10.1021/es802897x**.

This journal is © The Royal Society of Chemistry 2022

Environ. Sci.: Processes Impacts, 2022, **24**, 898–909 | **909**